

Glass transition in self organizing cellular patterns

Tomaso Aste* and David Sherrington

*Dep. of Physics, Oxford University, Theoretical Physics,
1 Keble R., Oxford OX1 3NP, England*

** INFN, C.so Perrone 24, Genova Italy and
LDFC, 3 rue de l'Université, Strasbourg France.
aste@infm.it*

July 2, 2021

Abstract

We have considered the dynamical evolution of cellular patterns controlled by a stochastic Glauber process determined by the deviations of local cell topology from that of a crystalline structure. Above a critical temperature evolution is towards a common equilibrium state from any initial configuration, but beneath this temperature there is a dynamical phase transition, with a start from a quasi-random state leading to non-equilibrium glassy freezing whereas an ordered start rests almost unchanged. A temporal persistence function decays exponentially in the high temperature equilibrating state but has a characteristic slow non-equilibrium aging-like behaviour in the low temperature glassy phase.

The hexagonal tiling is the best partition of the plane in equal cells. It solves both the packing and the covering problems. It is the space-filling assembly of equal cells with the minimal interfacial extension.

It is regular, perfect and beautiful. Surprisingly, however, it is never realized in natural biological tissues where a relevant amount of disorder is always present [1, 2]. This is reminiscent of the situation found in many covalently bonded solids, where, despite the lowest energy state being crystalline, in practice amorphous glassy structures are the common quasi-stable states [3]. Guided by this observation and by recent analysis of idealized infinite-ranged spin glasses[4] and in a desire to provide both a linkage to studies of covalent glasses and a minimalist model for understanding, we have studied the dynamics of the simplest ‘covalently bonded’ network subject to a simple stochastic dynamics characterized by a minimal set of control parameters, namely (i) deviations of local topology from crystalline and (ii) a temperature. The model has similarities with those of the classic works of Weber et. al.[5] and Wooten et. al.[6, 7], but complements and extends those studies by emphasising (and quantifying) not only the freezing of single time measures and slow relaxation, but also the apparent non-equilibrating non-stationary (aging) character of two-time correlation observables in the glassy phase. It therefore provides a link between the two fields of glass studies as epitomized by reference[4] on the one hand and references[5, 6] on the other. It should provide a valuable starting point for further theoretical analysis of systems complementary to those studied in[4] and in recent work on glass transitions in model systems with central forces[8]. It is also extendable, at least in principle, to higher dimensions/more-armed

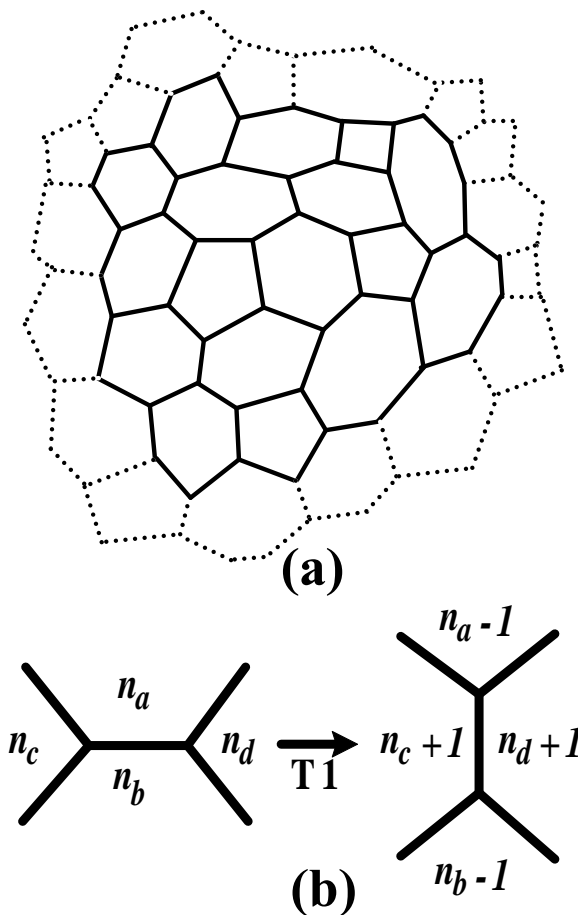


Figure 1: (a) A topologically stable cellular partition (froth). (b) A T1 move.

vertices. Our study combines Monte Carlo simulation and approximate analysis and concentrates on simple but novel one-time and two-time observables, introduced to probe issues of the character of those emphasised in[4].

In the hexagonal tiling each cell has six neighbours

and three cells meet at a common vertex. It is a regular two-dimensional, minimally-connected pattern. More generally we can consider disordered cellular patterns with 3-connected vertices such that the average number of sides per cell is 6 (Euler's theorem [2]). Locally, the degree of homogeneity can be measured in terms of the number of sides per cell. If n_i is the number of sides of cell i , then $q_i = 6 - n_i$ is a measure of its deviation from the hexagonal configuration. This quantity is the topological charge of the cell and is related to the local curvature. Local vertex re-arrangements conserve the total topological charge but allow migration and the annihilation of opposite charges on adjacent cells. When penalties are imposed for non-zero charges this mechanism leads the system to self organize.

Let us now turn to quantification. We characterize any structure by an 'energy' and consider random sequential stochastic dynamics driven by changes in that energy. The energy is a measure of the inhomogeneity in the structure. In the spirit of minimalism we

take it to be given by the ‘topological distance’ from the hexagonal lattice configuration:

$$E = \mu_2 N = \sum_{i=1}^N (q_i)^2 = \sum_{i=1}^N (6 - n_i)^2. \quad (1)$$

We consider a system conserving cell number (N). It evolves by T1 moves, which are topological transformations consisting of an exchange of neighbours between 4 cells [see fig.(1)]. Consider a T1 move performed on a system of four cells where the two adjacent cells have n_a and n_b sides and the two second neighbour cells have n_c and n_d sides respectively. After the T1 move, the cells with n_a and n_b sides lose one edge each, whereas the cells with n_c and n_d sides each gain an edge. The change of the energy associated with this move is

$$\Delta E(n_a, n_b; n_c, n_d) = 2(2 + n_c + n_d - n_a - n_b)$$

We consider dynamics of a Glauber-Kawasaki type, where the probability of this T1 move is given by

$$\begin{aligned} \Pi(n_a, n_b; n_c, n_d) &= \frac{1}{1 + \exp(\beta \Delta E(n_a, n_b; n_c, n_d))} \\ &\times (1 - \delta_{n_a,3})(1 - \delta_{n_b,3})(1 - \delta_{c,d}) \end{aligned} \quad (2)$$

This probability allows a dynamical evolution even at zero temperature ($\beta = \infty$) if it reduces the energy or leaves it unchanged. In Eq.(2) the first two δ -function terms have been introduced to exclude moves that generate two-sided cells. The last term forbids moves which generate cells which are self neighbours, preventing the formation of tadpoles. Thus neither two-sided nor single-sided cells can arise if not present at the start.

Before considering the dynamics, let us consider the predictions of equilibrium. The partition function is the sum over all the possible froths with Boltzmann weights. Some limitations apply on the accessible values of the n_i .

For instance, the average number of neighbours ($\langle n \rangle$) is fixed to be equal to 6 [2]. Moreover, two-sided cells are not admitted (therefore $n_i > 2$). Self-neighbouring cells are also not admitted (which trivially implies $n_i < N$), but also other less trivial combinations of n_i might be forbidden. In general, to find the sets of admissible $\{n_i\}$ which lead to possible froths is a very difficult task.

We approximate the partition function:

$$Z(\beta, \lambda, N) \simeq \prod_{j=1}^N \sum_{n_j=3}^{N-1} \exp[-\beta \sum_i (6 - n_i)^2 - \lambda \sum_i (6 - n_i)],$$

where λ is a Lagrange multiplier fixed by the constraint $\langle n \rangle = 6$. Correspondingly, the probability of an n -sided cell in the system is

$$p(n) \simeq p(6) \exp[-\beta(6 - n)^2 - \lambda(6 - n)]. \quad (3)$$

When $N \rightarrow \infty$ and $\beta = 0$, $\lambda = \ln(3/4)$ and $p(n) = 16/27(3/4)^n$, with $\mu_2 = 12$.

To study the dynamics we performed extensive computer simulations on froths with $N = 100172$ ($= 317^2$) cells and periodic boundary conditions. We started from two different systems: **(i)** a very disordered network, obtained by performing $10^4 N$ T1 moves on edges chosen at random from an ordered hexagonal seed; **(ii)** a perfectly ordered pattern (the

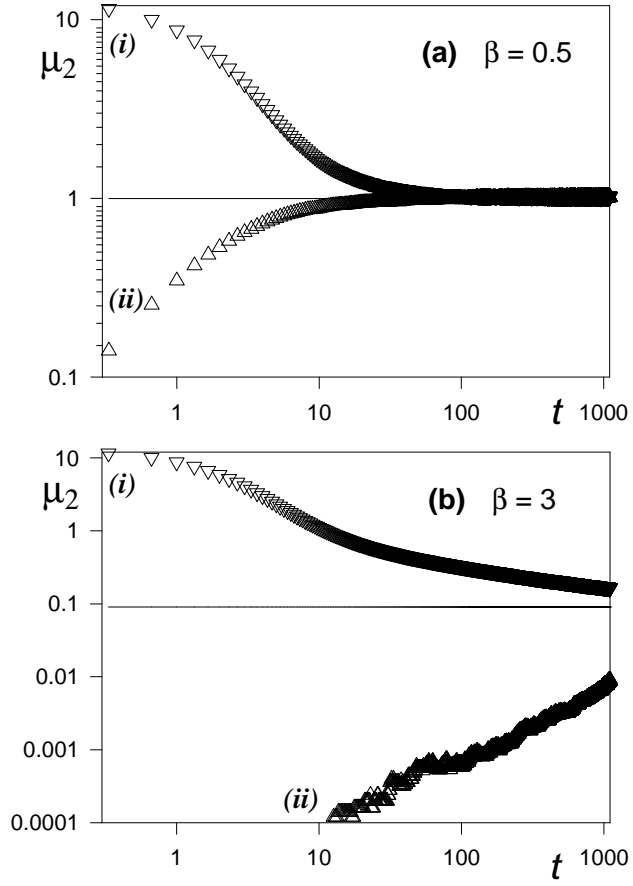


Figure 2: **(a)** μ_2 versus the number of attempted moves in units of N at $\beta = 0.5$ with starting configurations (i) and (ii) (triangles down and up). **(b)** $\beta = 3$. The lines are the theoretical predictions for thermodynamical equilibrium.

hexagonal tiling). In the simulation, $1100N$ T1 moves were attempted, with a probability given by Eq.(2), on edges chosen at random. First we consider a moderate-high temperature. In fig.(2a) μ_2 versus the number of attempted moves when $\beta = 0.5$ is shown for the two starting froths. These systems evolve from the two initial states (i) and (ii) with $\mu_2 \simeq 13$ and $\mu_2 = 0$ [9] respectively, toward a final equilibrium configuration with a common $\mu_2 \simeq 1$ reached after about $100N$ attempted moves. Second we turn to a lower temperature. In fig.(2b) μ_2 is plotted versus the number of attempted moves for $\beta = 3$. In this case, after $1100N$ attempted moves, the equilibrium configuration is not yet reached, the two patterns generated from the two initial states (i) and (ii) are still statistically different, and the approach toward a common equilibrium configuration is very slow.

In fig.(3) $p(n)$ and μ_2 are plotted for several simulations performed at different temperatures, starting from the two initial states (i) and (ii) and attempting $1100N$ moves. At high temperatures ($\beta^{-1} > 1$) the two final distributions $p(n)$ and μ_2 corresponding to the starting configurations (i) and (ii)

coincide and are in good agreement with the analytical prediction [9]. The system has reached thermodynamical equilibrium and we designate the state as a ‘liquid’. At low temperatures ($\beta^{-1} < 1$) the $p(n)$ and μ_2 reached do not coincide any more. The dynamics is slow and the system no longer reaches the thermodynamical equilibrium state in the time-scale studied. In the low temperature region for $T < O(1)$, an ordered start rests almost unchanged and a random start seems to lead to a freezing with $p(n)$ close to the form given by Eq.(3) with $\beta = 2.4$. Hence we identify $T_d \simeq (2.4)^{-1}$ as the dynamical freezing transition for the time-scale studied and we designate the corresponding metastable phase as a glass.

In order to better characterize these two different dynamics at high and low temperatures, we have also studied a *two time persistence function* $C(t_w + \tau, t_w)$ [11]. It counts the fraction of cells that have not been involved in a T1 move between the time t_w and $t_w + \tau$. In fig.(4) the persistence functions for $\beta = 0.5$ and 10^8 , are reported versus τ for several value of t_w . At high temperatures the persistence function appears time-translationally invariant and decays exponentially fast as in a *liquid*, whereas at low temperatures it shows a slow aging-like behaviour as in a *glass* [10, 4]. Thus, at low temperatures the system has not equilibrated, even though the single-time measures are no longer evolving significantly.

Let us now turn to theoretical expectations for C and consider a given cell i . The probability that between times t and $t + 1$ one of its edges or one of the edges incident on its vertices ($2n_i$ edges in total) is chosen (among the $3N$ edges in the system) to attempt a T1 move is $2n_i(t)/3N$. This T1 move is effectively performed with a probability $A_i(t)$ that depends on the local configuration as in Eq.(2). The probability that a given cell i is not involved in any move between the time t_w and $t_w + \tau$ is therefore

$$\begin{aligned} \overline{c_i(t_w + \tau, t_w)} &= \prod_{t=t_w}^{t_w+\tau} \left[1 - \frac{2n_i(t)}{3N} A_i(t) \right] \\ &\sim \exp \left[- \sum_{t=t_w}^{t_w+\tau} \frac{2n_i(t)}{3N} A_i(t) \right] \quad , \end{aligned} \quad (4)$$

and the expectation value of the persistence is $\overline{C(t_w + \tau, t_w)} = \sum_i \overline{c_i(t_w + \tau, t_w)}$.

At high temperatures in thermodynamical equilibrium we expect that the local configuration around the cell i evolves through a set of similar configurations typical of the whole system. Therefore, for large τ , $\sum_{t=t_w}^{t_w+\tau} 2n_i(t) A_i(t) \simeq 2\overline{nA}\tau$. This leads to a persistence func-

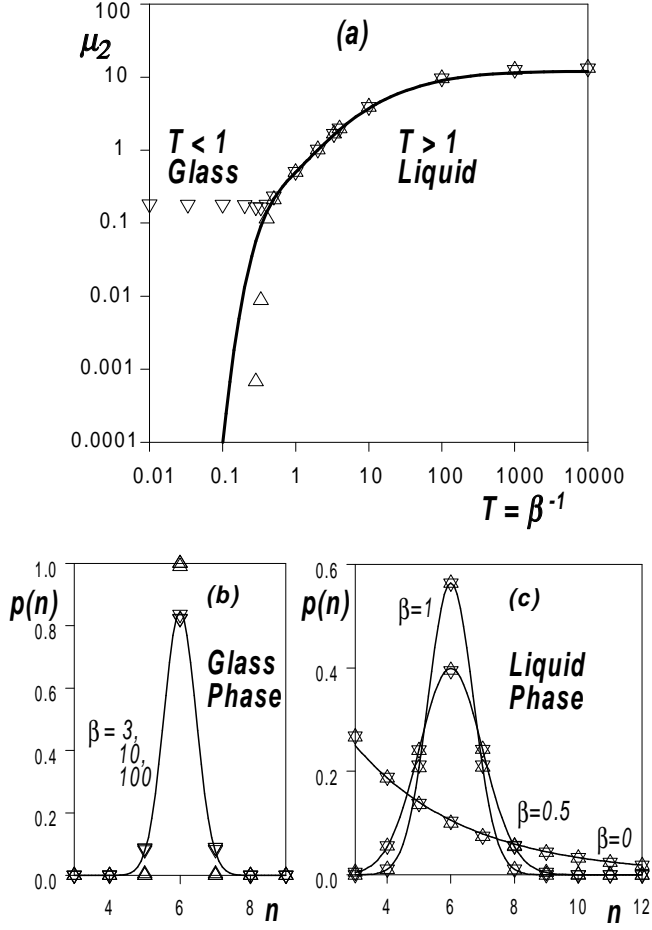


Figure 3: **(a)** μ_2 versus temperature ($T = \beta^{-1}$) with starting configurations (i) and (ii) (triangles down and up) dynamically equilibrated for $1100N$ moves. The full curve is the theoretical prediction at the thermodynamical equilibrium. **(b)** Side distributions ($p(n)$) at low temperatures in the “glass phase” ($\beta = 3, 10, 100$). The curve is the equilibrium prediction for $\beta = 2.4$. **(c)** Side distributions at high temperatures in the “liquid phase” ($\beta = 0, 0.5, 1$). The full lines are theoretical equilibrium predictions.

tion which is independent of t_w and decreases exponentially fast. This prediction is in good agreement with the results from simulations for $\beta \leq 1$ where we obtain best-fit values for \overline{nA} equal to 0.9, 0.83 and 0.42 for $\beta = 0, 0.5$ and 1 respectively.

At low temperatures, almost only 5, 6 and 7 sided cells are present in the system. We can restrict consideration to T1 moves which either leave the energy unchanged or reduce it. The former act to move pairs of 7-sided cells, pairs of 5-sided cells and 5-7 couples with adjacent pairs of 6-sided cells.

Pairs of 5-7 couples are brought together by this motion and annihilate to produce four 6-sided cells. The probability that between time t and $t + 1$ a 5-7 couple produces a T1 move in a given cell i is proportional to the number $M_{5|7}$ of 5-7 couples in the system: $\overline{nA} \propto M_{5|7}$.

The cellular pattern evolves reducing the number of 5-7 couples. This happens when two 5-7 couples are close together and a T1 move

annihilates both. The number of couples that annihilate per unit of time ($\frac{dM_{5|7}}{dt}$) is proportional to the probability for two couples to be close together which, ignoring correlations, is proportional to $(\frac{M_{5|7}}{N})^2$. This implies $M_{5|7} \propto (t + t_0)^{-1}$ and consequently $\sum_{t=t_w}^{t_w+\tau} 2n_i(t)A_i(t) \sim \alpha \ln(t_w + t_0 + \tau) - \alpha \ln(t_w + t_0)$, with α a coefficient which depends on the details of the annihilation process. By substituting into Eq.(4), we get $\overline{C(t_w + \tau, t_w)} \sim C_0(\frac{t_w + t_0}{t_w + t_0 + \tau})^\alpha$. In fig.(4) this expression is compared with the results from the simulations for $\beta = 10^8$. When $t_w < 10N$ the behaviour of the persistence function is in good qualitative agreement with this crude theoretical prediction with fit parameters $\alpha \simeq 2.5$, $t_0 = 2N$ and $C_0 = 1$, but for large waiting times $t_w > 100N$ the dynamics become slower.

In fact the recent spin-glass work[4] emphasises that aging in two-time quantities continues for both waiting time t_w and relative time τ much greater than the characteristic settling time-scale for one-time quantities. Hence it would be of interest to extend these studies to much longer run-times, as well as to higher dimensions.

In summary, in a minimalist model of a continuous network subject to stochastic dynamics determined by a simple local topological ‘energy’ and a randomizing temperature we have identified a dynamical phase transition and have distinguished two phases: “*liquid*” at high temperatures and “*glass*” at low temperatures. The dynamics is *fast* and equilibrating from any starting state in the *liquid* phase and *slow* and *aging* in the *glass* phase which is achieved from a random starting state. In our explicit characterization the dynamics become slow for $\beta < 1$ and the transition to the glass phase is around the point $\beta = 2.4$.

Although the micro-dynamics we have considered is idealized and chosen for minimalist study, it is interesting to compare our results with those observed in nature. Most undifferentiated biological tissues are space-filling assemblies of cells where the side distribution is centered around $n = 6$ and the second moment μ_2 takes values between 0.5 and 1.2; for instance, $\mu_2 = 0.53$ in *human epidermis* [12], $0.6 \leq \mu_2 \leq 1.1$ in vegetable leaves [13], $\mu_2 = 0.68$ in *cucumber epithelia* and $\mu_2 = 1.00$ in *human amnion* [1].

We have found slow dynamics in systems with low amount of disorder ($\beta > 1$ and $\mu_2 < 0.5$) and fast dynamics in systems with higher disorder ($\beta < 1$ and $\mu_2 > 0.5$). One might speculate that the ‘ideal’ biological tissue must fit the compromise between low disorder (homogeneity) and

fast dynamics (efficient recovering of perturbations), implying a structure with a value of μ_2 a little above 0.5.

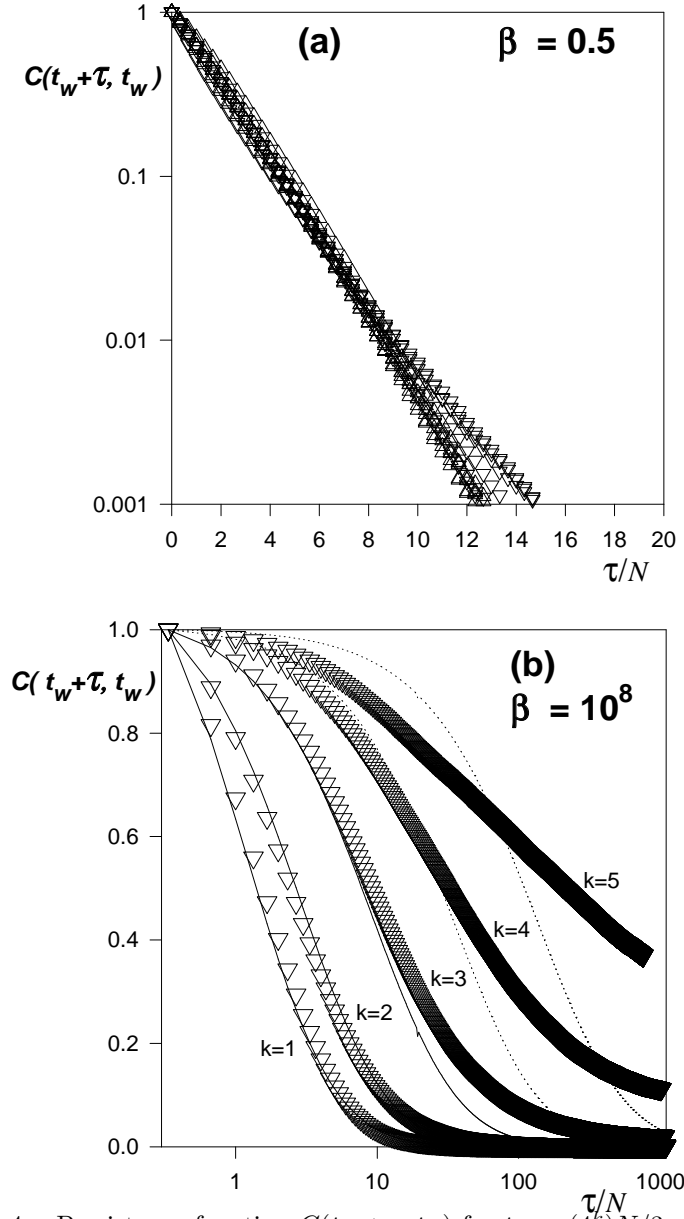


Figure 4: Persistence function $C(t_w + \tau, t_w)$ for $t_w = (4^k)N/3$ with $k = 1, \dots, 5$. **(a)** At high temperatures ($\beta = 0.5$) the persistence function is independent of t_w and decreases exponentially fast. **(b)** At low temperatures ($\beta = 10^8$) $C(t_w + \tau, t_w)$ depends on t_w and shows a slow decay. The curves correspond to fits of the form $C(t_w + \tau, t_w) \sim C_0 (\frac{t_w + t_0}{\tau})^\alpha$ with $\alpha = 2.5$, $t_0 = 2N$ and $C_0 = N$.

Acknowledgements

T. Aste acknowledges partial support from the European Council (TMR contract ERBFM-BICT950380). A special thanks to Helgo Ohlenbuch who wrote the original C code which has been modified and used for the present simulations.

References

- [1] F. T. Lewis, *Anat. Rec.* **50** (1930) 235.
- [2] D. Weaire and N. Rivier, *Contemp. Physics* **25** (1984) 59.
- [3] W.H. Zachariesen, *J.Am Chem Soc.* **54**, (1932) 3841
- [4] J.P. Bouchaud, L. Cugliandolo, J. Kurchan and M. Mézard, in *Spin Glasses and Random Fields*, Ed. A.P. Young (World Scientific, Singapore, 1998)
- [5] T.A. Weber, G.H. Fredrickson and F.H. Stillinger, *Phys. Rev. B* **34**, 7641 (1986);
T.A. Weber and F.H. Stillinger, *Phys. Rev. B* **36**, 7043 (1987)
- [6] F. Wooten, K. Winer and D. Weaire, *Phys. Rev. Lett.* **54**, 1392 (1985)
- [7] see also ref ([2])
- [8] M. Mézard and G. Parisi, cond-mat/9807420
- [9] The difference between the observation of $\mu_2 = 13$ and the theoretical estimate of 12 presumably reflects the approximations made in the partition function. At infinite temperatures ($\beta = 0$) the topological constraints have a major importance and must be treated with more care (see for instance, E. Brézin, C. Itzykson, G. Parisi and J.B. Zuber, *Commun.math. Phys.* **59** (1978) 35.).
- [10] L.C.E. Struik, *Physical aging in amorphous polymers and other materials* (Elsevier, Houston 1978)
- [11] B. Derrida, V. Hakim and V. Pasquier, *Phys. Rev. Lett.* **75** (1995) p. 751.
Geometries
- [12] B. Dubertret and N. Rivier, *Biophysical Journal* **73** (1997) 38-44.
- [13] J.C.M. Mombach, M.A.Z. Vasconcellos and R.M.C. de Almeida, *J. Phys. D Appl. Phys.* **23** (1990) 600-606.